Internal magnetic pitch angle measurements at KSTAR tokamak

J. Ko [a*], J. Chung [a], M. C. C. Messmer [b]
[a]*National Fusion Research Institute,169-148 Gwahak-Ro, Daejeon 305-806, Republic of Korea*
[b]*Eindhoven University of Technology, P. O. Box 513, 5600 MB Eindhoven, The Netherlands*
[*]*Corresponding author: jinseok@nfri.re.kr*

1. Introduction

A PEM (Photo Elastic Modulator) based polarimetric motional Stark effect (MSE) system is under development for the KSTAR tokamak [1]. The conceptual design is almost complete for the optics design, the filter selection, and the number of channels (spatial resolution and coverage). Specification of the hardware for photo-detecting and digitizing electronics has almost complete as well and many of them are ready for procurement. The main collaboration party is Eindhoven University of Technology in the Netherlands, whose main responsibilities include the development of filter module design and off-line & real-time analysis schemes along with overall consultations. The following sections describe some major parts of the design progress.

Table I: Problem Description

Machine		Δr/a (%)		Number of channels
		min	max	
ITER		2.5	8	20
JET		2	6	25
JT-60U		8	10	16
DIII-D	15T	38	23	10
	315T	1.5	15	16
	195TL	8	11	8
	45T, 195TU	< 1.5	8	9, 16
NSTX		3	5	12
C-Mod		10	40	10
MAST		5	5	35
KSTAR		2	6*	30

2. Spatial and time resolutions

The ITER MSE requirements specify the radial resolution of $\Delta r/a \approx 5\%$ with 20 channels in order to obtain reasonable q profiles for NTM feedback (q = 1.5, 2) and reversed shear control [2]. Keeping this number in mind, Table 1 summarizes and compares the radial resolution of the MSE system for various machines around the world. The radial resolution becomes poorer rapidly as the view passes through the magnetic axis and goes inward as shown in Figure 1, where the point-spread-function, or the radial resolution, calculated from the emission profiles of the MSE lines of sight across the beam and projected onto the major-radius axis is shown. The actual radial resolution ranges from 1 to 2 cm over most of the MSE coverage (R = 1.74 – 2.28 m) except for one innermost channel or two (about 3 cm). Nonetheless, we would like to cover at least 10 ~ 20 % minor radius inside the magnetic axis to explicitly and directly measure the safety factor on the magnetic axis, q0.

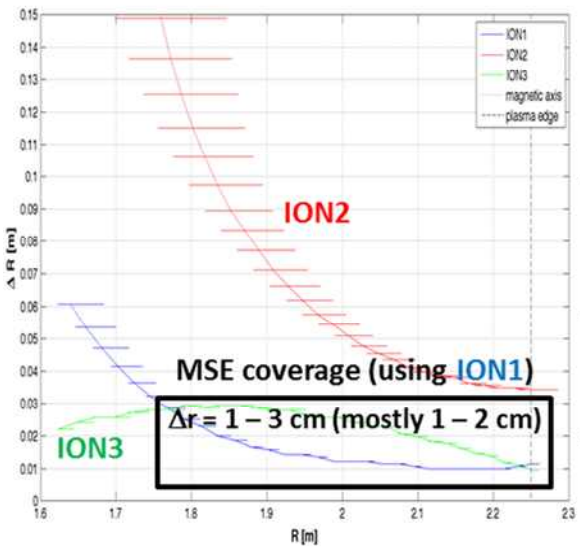

Fig. 1. Point-spread-function, or radial resolution for the three ion sources from NBI1 as a function of major radius.

Theoretically, MSE time resolution is limited by the PEM fundamental frequencies (~ 20 kHz). Practically, however, it is limited by the amount of photons from the beam emission. This is typically several tens of msec. The MSE systems using high power heating beams have very high measurement speed. The DIII-D MSE, for instance, is able to measure the magnetic fluctuation associated with a resistive wall mode rotated by internal coils at 20 Hz in its normal operation mode [3]. The typical H-mode energy confinement time in KSTAR $\approx 1.4a^2\kappa Te^{1.5}$ (keV)/Zeff $\approx 1.4 \times (0.5)^2 \times 1.8 \times 2^{1.5} / 2 \approx 1$ sec [4]. The real time equilibrium reconstruction planned for KSTAR discharges can tolerate as low as 50 Hz. These three time scales seem to make ~ 10 msec time integration of the KSTAR MSE signals reasonable.

3. Design of front optics

There are several challenging issues in designing the front optics that collect the light after the vacuum window at the midplane M-port of the KSTAR tokamak.

The most difficult one is to share the collection optics with another diagnostic system, Charge Exchange Spectroscopy (CES) in a 'cassette' structure inserted into the port. The CES utilizes the Doppler shifted Carbon line emissions around 550 nm to measure the temperature (Doppler broadening), velocity (Doppler shift), and density (the amount of emission) of the Carbon impurity in the plasma. This diagnostic has occupied the midplane M-port for several years, producing good data. By adding the photo-elastic modulator and a polarizer, the attenuation of the input light can take place. To avoid the degradation of the CES signal strength, a dichroic beam splitter that transmits the light below 600 nm for CES and reflects the light above 600 nm for MSE. Figure 2 illustrates this splitting of the signals in the 3D layout of the front optics model.

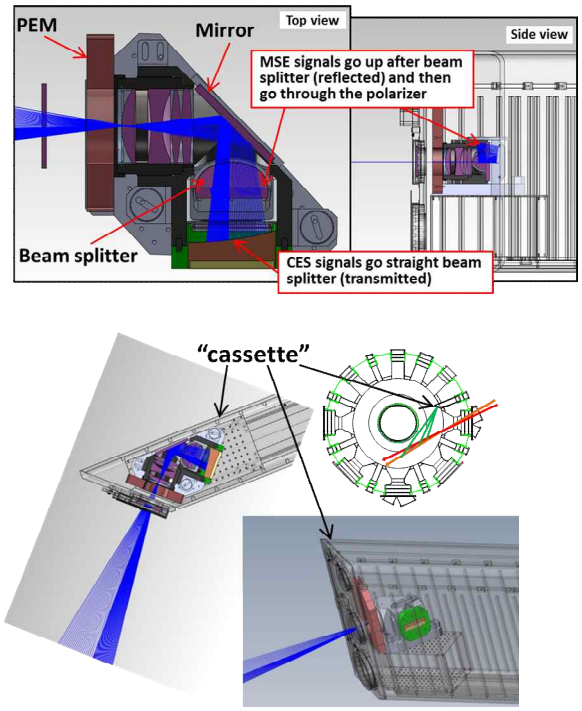

Fig. 2. 3D model of the MSE front optics installed in the M-port cassette.

The polarization properties of polarized light, when reflected, can be changed. The P- and S-polarization components with respect to the plane of incidence have their own phase and reflectivity and their response to the reflection are different to each other. Normal reflectors would cause more than a few degrees of error in the pitch angle measurements. Therefore, it is critical to minimize the relative phase shift (close to 0° or 180°) and reflectivity (close to 1) between the P- and S-polarizations at the wavelength of interest (~ 650 nm) and angles of incidence (35 - 55° at the mirror and 40 - 50° at the beam splitter). This 'extreme' performance can be achieved by a special dielectric coating using ion beam sputtering technology. Figure 3 shows such a performance for the mirror and the beam splitter suggested by the vendor (MLD Tech, USA). It is expected that for the MSE wavelengths and angles-of-incidence, the S/P reflectance ratio is 1 ± 0.1% and the phase difference is within 5°. Large deviations with angles-of-incidence outside the operation range (dashed lines in Figure 3) indicate how extreme and difficult such a phase-control coating design is.

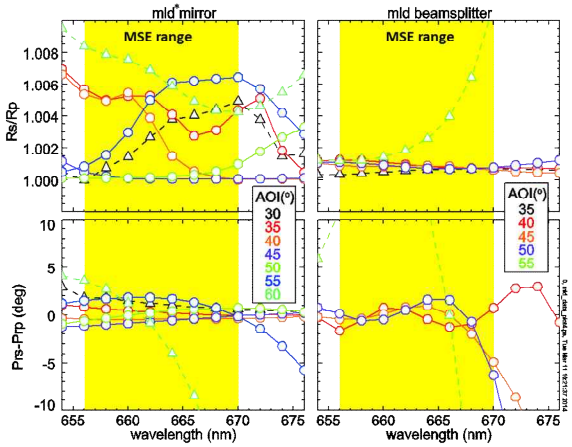

Fig. 3. Designed performance of the mirror and the beam splitter.

4. Design of filter modules

3D MSE stokes-vector simulations have been tuned to match the MSE spectra measured in KSTAR and used to design the band-pass filters. From these simulations, 0.4-nm 2-cavity interference filters have been chosen to minimize pitch angle errors. Figure 4 shows an example of the MSE spectrum calculated from the simulation that is compared with the measured spectrum. Also shown in Figure 4 are the possible pass-band (shaded in green) of the spectrum where the red-most shifted polarization component ($+4\pi$) is chosen, the pitch angles and their errors. Due to the overlap of the spectra among ion sources, the second ion source of NBI1 (NBI1-2) should operate at about 15% lower voltage than that of the first ion source (NBI1-1). An example of this overlap in the spectrum and the large error in pitch angle it causes is shown in Figure 5.

Pass-band control by the filter-angle tuning is under development to fully cover most of the KSTAR plasmas which include Ip = 0.5 ~ 1 MA, Bt = 1.5 ~ 3.5 T, and the beam energy (for the ion source 1 from NBI1) = 70 ~ 100 keV. Motorized rotation stages will be used for this purpose. There is a standard client tool available to control the motor angle using the engine controller. However, custom software has been implemented to tune the filter, using the available ActiveX component. With the new customized control, it is possible to tune the filter according to its central wavelength and not to its angle, which is necessary for the MSE diagnostic. The accuracy obtained is in the order of 0.5 % and

compatible with the MSE requirement. The software also allows sequences creation, which consists of executing a series of a predefined central wavelength and a corresponding time delay. One PC can control 5 controller hubs each of which can accommodate up to 6 rotational stage/controller sets, resulting in the maximum 30 sets.

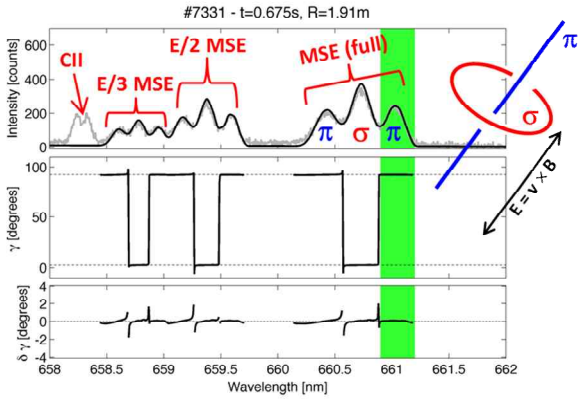

Fig. 4. (TOP) Comparison of simulated and measured beam emission spectra from the first source of NBI1 (80 keV). (MIDDLE) Corresponding polarization angle spectrum. (BOTTOM) The systematic deviation of the polarization angle.

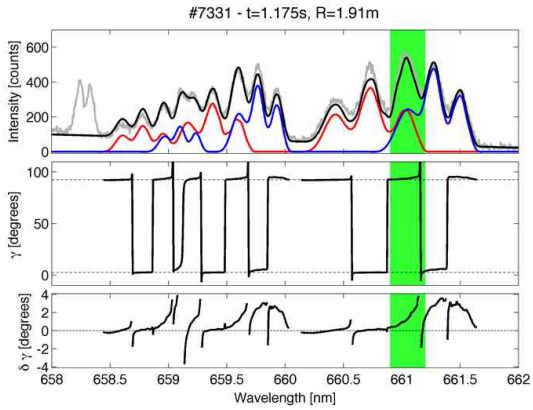

Fig. 5. (TOP) Comparison of simulated and measured beam emission spectra from NBI1-1 (80 keV) and NBI1-2 (90 keV). (MIDDLE) Corresponding polarization angle spectrum. (BOTTOM) The systematic deviation of the polarization angle.

REFERENCES

[1] J. Chung, J. Ko, M. F. M. De Bock, R. J. E. Jaspers, Instrumentation for a multichord motional Stark effect diagnostic in KSTAR, Rev. Sci. Instrum. 85, 11D827, 2014

[2] A.J.H. Donne, A.E. Costley, R. Barnsley, H. Bindslev, R. Boivin, G. Conway, R. Fisher, R. Giannella, H. Hartfuss, M.G. von Hellermann, E. Hodgson, L.C. Ingesson, K. Itami, D. Johnson, Y. Kawano, T. Kondoh, A. Krasilnikov, Y. Kusama, A. Litnovsky, P. Lotte, P. Nielsen, T. Nishitani, F. Orsitto, B.J. Peterson, G. Razdobarin, J. Sanchez, M. Sasao, T. Sugie, G. Vayakis, V. Voitsenya, K. Vukolov, C. Walker, K. Young, the ITPA Topical Group on Diagnostics, Chapter 7: Diagnostics, Nucl. Fusion 47, S337-S384, 2007

[3] R.J. Jayakumar M. A. Makowski, S. L. Allen, M. E. Austin, A. M. Garofalo, R. J. LaHaye, H. Reimerdes, T. L. Rhodes., Observation of magnetohydrodynamic instability and direct measurement of local perturbed magnetic field using motional Stark effect diagnostic, Rev. Sci. Instrum. 75, 2995, 2004

[4] P.T. Bonoli, , J. Ko, R. Parker, A. E. Schmidt, G. Wallace, J. C. Wright, C. L. Fiore, A. E. Hubbard, J. Irby, E. Marmar, M. Porkolab, D. Terry, S. M. Wolfe, S. J. Wukitch, the Alcator C-Mod Team, J. R. Wilson, S. Scott, E. Valeo, C. K. Phillips and R. W. Harvey, Lower hybrid current drive experiments on Alcator C-Mod: Comparison with theory and simulation, Phys. Plasmas 15, 056117, 2008